

ORBIT: An Object Property Reasoning Benchmark for Visual Inference Tasks

Abhishek Kolari¹, Mohammadhossein Khojasteh¹, Yifan Jiang², Floris den Hengst¹, Filip Ilievski¹

¹Department of Computer Science, Faculty of Science, Vrije Universiteit Amsterdam

²Information Sciences Institute, University of Southern California

a.v.kolari@student.vu.nl, m.khojasteh@vu.nl, yifjia@isi.edu, f.den.hengst@vu.nl, f.ilievski@vu.nl

Abstract

While vision-language models (VLMs) have made remarkable progress on many popular visual question answering (VQA) benchmarks, it remains unclear whether they abstract and reason over depicted objects. Inspired by human object categorisation, object property reasoning involves identifying and recognising low-level details and higher-level abstractions. While current VQA benchmarks consider a limited set of object property attributes like size, they typically blend perception and reasoning, and lack representativeness in terms of reasoning and image categories. To this end, we introduce a systematic evaluation framework with images of three representative types, three reasoning levels of increasing complexity, and four object property dimensions driven by prior work on commonsense reasoning. We develop a procedure to instantiate this benchmark into ORBIT, a multi-level reasoning VQA benchmark for object properties comprising 360 images paired with a total of 1,080 count-based questions. Experiments with 12 state-of-the-art VLMs in zero-shot settings reveal significant limitations compared to humans, with the best-performing model only reaching 40% accuracy. VLMs struggle particularly with realistic (photographic) images, counterfactual reasoning about physical and functional properties, and higher counts. ORBIT points to the need to develop methods for scalable benchmarking, generalize annotation guidelines, and explore additional reasoning VLMs. We make the ORBIT benchmark and the experimental code available to support such endeavors.

Code — <https://github.com/AbhishekKolari/ORBIT>

Introduction

Object representation and reasoning is one of the core systems of human cognition (Spelke and Kinzler 2007). By abstracting object properties and interactions, humans, including infants with limited real-world knowledge and experience, represent their environment and perform inference (Lipton and Spelke 2004). Object representation and reasoning in humans are driven by spatio-temporal principles of cohesion (objects move as connected and bounded wholes), continuity (objects move on connected, unobstructed paths), and contact (objects do not interact at a distance). Humans perceive object boundaries, represent object

Copyright © 2026, Association for the Advancement of Artificial Intelligence (www.aaai.org). All rights reserved.

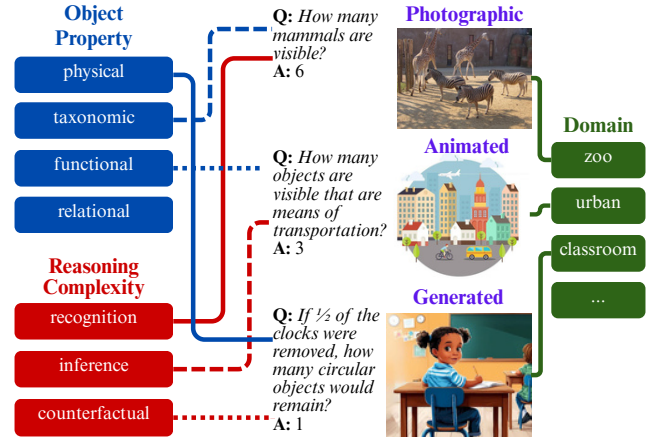


Figure 1: Visual question answering in ORBIT, with questions about different **object properties** of varying **reasoning complexity** on three **types of images** from different **domains**.

shapes that move (partially) out of view, and predict object movement (Aguir and Baillargeon 1999; Leslie and Keeble 1987). Object perception and inference is not merely descriptive; it involves a multi-stage process from low-level recognition, through categorization, to identification and reasoning (Fields 2016). For instance, to count how many mammals are visible in Figure 1-top, humans recognize the image objects, decide which of them fit the constraint (type) of a mammal, and count the ones that satisfy this criterion.

Recent work on the connection between perception and reasoning has used visual question answering (VQA) in natural language as a diagnostic task for vision-language models (VLMs). Prior work has developed VQA benchmarks for recognition of basic visual elements such as physical attributes or taxonomic category membership (Yuan et al. 2021; Tong et al. 2024), inference of relational properties (Lu et al. 2022; Hudson and Manning 2019), and counterfactual reasoning (Frohberg and Binder 2021; Yu et al. 2023; Li et al. 2024). As objects are central components of images, solving these benchmarks relies on various physical and abstract object properties (Johnson et al. 2017; Hudson and Manning 2019; Acharya, Kafle, and Kanan 2018).

Current benchmarks exhibit two key limitations. The first

Category		VQAv2	CLEVR	TallyQA	SCIENCEQA	GQA	C-VQA	CFMM	ORBIT
Counting Question		✓	✓	✓		✓	✓	✓	✓
Object Properties	Physical	✓	✓	✓	✓	✓	✓	✓	✓
	Taxonomic				✓	✓			✓
	Functional				✓				✓
	Relational		✓	✓		✓		✓	✓
Image Types	Real	✓	✓	✓	✓	✓	✓	✓	✓
	Animated				✓				✓
	AI-Generated								✓
Reasoning Complexity	Direct Recognition	✓	✓	✓	✓	✓	✓	✓	✓
	Property Inference				✓	✓			✓
	Counterfactual						✓	✓	✓

Table 1: **ORBIT** versus VQAv2 (Goyal et al. 2017), CLEVR (Johnson et al. 2017), TallyQA (Acharya, Kafle, and Kanan 2018), SCIENCEQA (Lu et al. 2022), GQA (Hudson and Manning 2019), C-VQA (Zhang et al. 2024b), and CFMM (Li et al. 2024).

limitation is the lack of a delineation between the separate subtasks that comprise object perception and reasoning, namely, object recognition, inference, and counterfactual reasoning. While some works have identified small object sizes and peripheral locations as causes of failure in VLMs (Zhang et al. 2025, 2024a), the lack of separation between these subtasks prevents comprehensive diagnostics of the VLMs’ strengths and weaknesses. Second, current benchmarks are often limited in *representativeness* of the attributes, as most benchmarks are limited to basic features such as shape and color. While Jiang et al. (2024) recently proposed a systematic benchmark for abstract visual reasoning, it relies on manipulating simple shapes in synthetic environments with minimal noise. Meanwhile, the ability of VLMs to perceive and reason over real-world objects and across image types remains underexplored.

We address this gap in the understanding of the capabilities of current models with *a structured and comprehensive evaluation of the ability of VLMs to perceive and reason about a range of property relations of objects using counting questions in three image types*. We make three contributions, which are illustrated in Figure 1: 1. **A systematic evaluation framework** for object property reasoning, consisting of three image types, three levels of reasoning complexity, and four dimensions of commonsense knowledge. 2. **A semi-automatic** procedure for dataset creation and the **ORBIT** VQA benchmark with 1,080 high-quality counting questions about 360 images. 3. **An extensive experimental analysis** of a wide range of state-of-the-art VLMs on ORBIT, revealing current models’ limitations compared to humans, especially for photographic images, counterfactual reasoning, functional knowledge, and higher counts.

Related Work

Object Properties in Visual Question Answering. VQA has long served as a diagnostic task for evaluating the visual and reasoning capabilities of AI systems. Early efforts (Antol et al. 2015; Goyal et al. 2017) emphasized general visual recognition of objects, colors, and basic attributes, while subsequent benchmarks (Singh et al. 2019; Mathew, Karatzas, and Jawahar 2021; Lu et al. 2022) tar-

geted domain-specific context. Although many benchmarks across domains (Johnson et al. 2017; Hudson and Manning 2019; Acharya, Kafle, and Kanan 2018) require reasoning over object properties, none of them provide a systematic separation of object property dimensions. Compared to previous VQA benchmarks, ORBIT covers four distinct object dimensions based on commonsense resources (Speer, Chin, and Havasi 2017; Ilievski et al. 2021; Kurtz and Silliman 2021): physical, taxonomic, functional, and relational, and enables fine-grained assessment of object-level reasoning as visualized in Table 1.

Reasoning Complexity in Visual Understanding. Human cognition is inherently compositional, and integrates multiple scene aspects into higher-level reasoning, with complexity progressing from direct recognition to property-level inference, and counterfactual reasoning (Hoffman and Richards 1987; Xu, Huang, and Liu 2021). Initial *direct recognition* is limited to recognition of basic visual elements such as physical attributes or taxonomic category membership (Yuan et al. 2021; Tong et al. 2024). *Inference* builds on recognition, targets higher-level functional or relational properties, and requires multi-step abstraction beyond surface-level features (Lu et al. 2022; Hudson and Manning 2019). *Counterfactual reasoning* involves reasoning about hypothetical changes made in inputs. This type of reasoning is most challenging as it requires understanding and adapting to hypothetical, altered, or out-of-context scenarios (Frohberg and Binder 2021; Yu et al. 2023; Li et al. 2024). Various benchmarks have been proposed to target different types of reasoning (Table 1), yet none of them provide a systematic evaluation across all types simultaneously. In contrast, ORBIT is the first to encompass all three reasoning types and extends evaluation to three image domains, and thereby enables a more comprehensive assessment of models’ reasoning abilities in visual understanding.

A Framework for Object Property Evaluation

We devise a systematic framework for rigorous evaluation of VLMs, integrating object property dimensions (physical, taxonomic, functional), levels of reasoning complexity (recognition, property inference, counterfactual reasoning),

and a variety of image types (photographic, animated, AI-generated). We next detail the three framework components.

Object Property Dimensions

Drawing on prior research (Ilievski et al. 2021; Tandon, de Melo, and Weikum 2017) on representing commonsense knowledge about properties and their relations, our framework distinguishes four object property dimensions relevant for count-based VQA. Each dimension captures a distinct facet of human conceptualization and reasoning about objects, their attributes, and relations in visual scenes.

Physical knowledge refers to the dynamics of physical systems based on observable phenomena and fundamental principles (McCloskey, Washburn, and Felch 1983) (e.g., *circular objects* in Figure 1). Our framework enhances the list of physical properties in prior work, such as shape, color, and size (Table 1), with more complex attributes like the *material* (wood, metal), *state* of the object (liquid, solid), and structural characteristics of the object – including part-whole relationships such as *has wheels* and *has legs*. Physical properties, such as object qualities, materials, and part-whole relations, are prevalent in commonsense knowledge representation (Tandon, de Melo, and Weikum 2017; Fleming 2017).

Taxonomic knowledge captures an object’s semantic category or class membership, typically expressed as *is-a* relations (Ilievski et al. 2021). Examples include broad ontological groupings such as *biological* (e.g., mammals, reptiles), *artifact* (e.g., furniture, tools), and *food* (e.g., fruits, vegetables) categories. Unlike physical attributes, taxonomic properties may not be visible from visual input alone. To determine how many mammals are present in an image (Figure 1), for example, visual identification of species needs to be combined with knowledge of their categorization. The taxonomic dimension aligns with *taxonomic semantic systems* from cognitive science and domain-specific knowledge representation, which group entities based on shared features and categorical similarity (Mirman, Landrigan, and Britt 2017). Taxonomic groupings are also linguistically supported: for instance, Lobben (2012) showed their universality based on similarities in the noun class system of roughly 500 languages in the Bantu language family.

Functional properties express capabilities and general design aspects of an object. This includes attributes such as *utilities* and *capabilities* of an object (e.g., means of transportation in Figure 1), *affordances* as actions an object receives (e.g., breakable, foldable), and *operational dependencies* for an object to function (e.g., electricity, battery). This dimension primarily aligns with the *utility* and *causal* relations identified in commonsense knowledge frameworks (Speer, Chin, and Havasi 2017; Heindorf et al. 2020; Ilievski et al. 2021). Questions about the utility of objects have been included in prior VQA literature (Table 1): for example, the OK-VQA benchmark (Marino et al. 2019) tests for knowledge about implicit functionality based on utility, e.g., recognizing that *a broom* is for *sweeping*.

Relational knowledge captures how objects interact, how they can be grouped, and how they are situated relative to one another within a visual context. Attributes include *spatial relationships* (e.g., on top of, hanging from) and *group-*

ing relations (e.g., couple, flock). Questions like “*How many couples are visible?*” or “*How many objects can be seen hanging from the wall?*” evaluate a model’s ability to reason about such properties. The relational dimension is motivated by the *spatial* and *relational-other* relations in commonsense reasoning (Ilievski et al. 2021). It is limited to spatial and contextual groupings of instances, making it complementary to the internal relations of objects in part-whole relationships in the physical dimension and taxonomic groupings in the taxonomic dimension.

Reasoning Complexity

The four object property dimensions can support questions with various levels of complexity. We introduce three levels of reasoning complexity: *direct recognition*, *property inference*, and *counterfactual reasoning*, exemplified in Figure 1. We expect that the progression from direct recognition to counterfactual reasoning requires an increasingly high level of abstraction to answer a question, thus increasing in difficulty (Xu, Huang, and Liu 2021).

Direct Recognition questions are features that can be detected by observation and general categorical knowledge. Questions at this level can be recognized through an atomic step of perception and reside at the physical and taxonomic property dimensions. Since answers can be derived from specific visual regions or patterns, recognition questions primarily assess object recognition abilities, e.g., the top question in Figure 1 only requires identifying land animals and categorizing them as mammals.

Property Inference questions are targeted at the functional and relational property dimensions, which require deeper abstraction, introducing multi-step reasoning. Due to the properties having codependencies among objects and underlying relations across different image regions, this would push models to generalize beyond surface-level features. For example, in Figure 1, the middle question requires identifying a bicycle, a car, and a plane, categorizing them as vehicles, and then reasoning about their utility in transportation.

Counterfactual Reasoning questions probe the VLM’s ability to reason about hypothetical, altered, or out-of-context scenarios. Counterfactual questions span any of the four property dimensions. In addition to visual recognition and inference, counterfactual questions also require commonsense knowledge and flexible abstraction (e.g., creating a contextualized procedure that identifies remaining circular objects besides half of the clocks in the bottom question of Figure 1), which makes them the most complex of the three reasoning categories in our framework.

Image Types

To evaluate VLM generalization across visual domains, we incorporate a diverse set of image types, recognizing that model performance may vary (and typically worsen) when moving from synthetic to real-world images (Johnson et al. 2017; Hudson and Manning 2019).

Photographic images represent naturalistic settings, featuring complex textures, lighting variations, and cluttered scenes. They are realistic, i.e., all depicted objects are encountered in the real world. Photographs present challenges

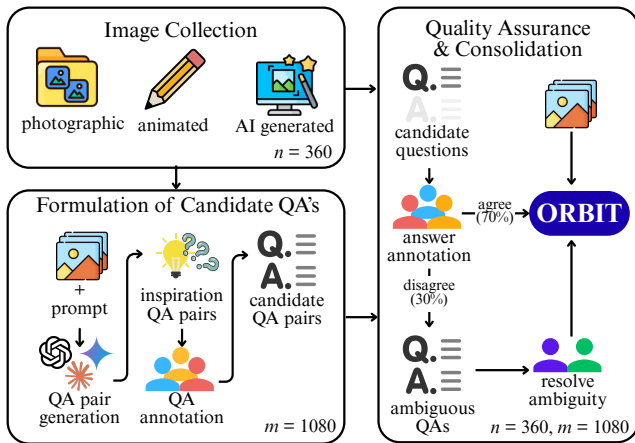


Figure 2: ORBIT construction pipeline: image collection, candidate QA formulation, and quality assurance. n and m stand for number of images and questions, respectively.

like occlusions, viewpoint variation, and natural ambiguity, demanding a high level of visual grounding from models.

Animated images are simplified or stylized and contain minimal visual noise, as well as limited levels of detail when compared to photographic images. Humans typically create animated images in a digital format, and their objects may or may not be realistic. Object boundaries in animated images may be easier to detect, but exaggerated representations may pose a novel challenge.

AI-generated images include both photorealistic and stylized images, created by prompting generative models. These images test a model’s robustness to domain shifts, as they may deviate from typical real-world physics, object proportions, and other visual conventions. AI-generated images typically feature simpler compositions and include objects that are implausible in practice, such as half-animals or glasses floating in the air.

ORBIT Benchmark Construction

Our dataset curation follows a three-phase pipeline (Figure 2). We *collect images* from public sources corresponding to the three image types. Then, we ask an annotator to *formulate candidate question-answer* pairs for all images, inspired by AI-generated questions. Then, the questions and answers undergo additional rounds of human refinement for *quality assurance*. The outcome of these steps is assembled in the last phase as ORBIT, where we present statistics about the benchmark content. We detail each step below.

Image Collection. To ensure diagnostic quality and mitigate data contamination risks from existing benchmarks (Dodge et al. 2021), a collection of previously unsourced images is created. We pick 15 themes grouped into three categories from the McGyver dataset (Tian et al. 2025), and add additional 11 for a total of 26 themes (see Table 7 for the complete list). The three broad categories, defined in (Tian et al. 2025), are: indoors/household (e.g., kitchen), neutral (e.g., garage), and outdoors (e.g., zoo). We use these themes as queries for all three image types, which facilitates direct

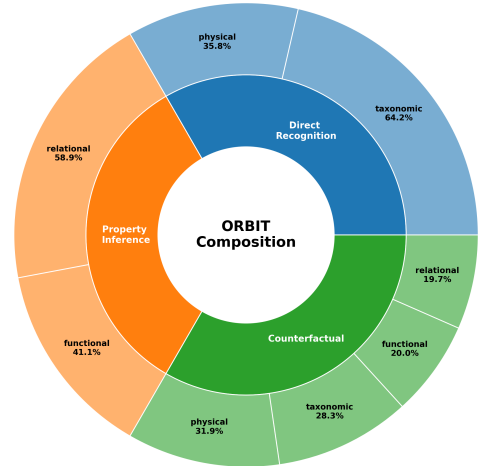


Figure 3: ORBIT question composition in percentages.

comparisons between images of comparable scenes. We collect public images by querying a variety of sources: Google Images, Unsplash, and Freepik for photographic and animated images; GPT-4o and Grok3 for AI-generated ones (example generative AI prompts are provided in Table 8). We explicitly exclude diagrammatic images (Lu et al. 2022). In total, we collect 360 images (120 per type).

Formulation of Candidate QA-pairs. We formulate initial question-answer pairs using a semi-automatic procedure. Namely, we prompt an MLLM to generate three questions (one per reasoning level) following the framework defined in the previous section. The MLLM is selected at random from three closed-source models: GPT-4o (OpenAI et al. 2024), Claude 3.7 Sonnet (Anthropic 2025), and Gemini 2.0 Flash (Google et al. 2025a). The resulting 1,080 question-answer pairs are then leveraged by human annotators, instructed to revise or replace the questions and answers to ensure high quality. Namely, humans ensure that the question is precise and it fits the restrictions of our evaluation framework, as well as that the answer count is not too high (we cap the answers to a maximum of 10). A pool of five annotators annotates the images, each responsible for 72 images. When possible, the annotators are instructed to abstract away from the specific object types, e.g., to use “how many objects are made of rubber” instead of “how many tires are made of rubber?”. In practice, the annotators rewrote a vast majority of the questions, and nearly all answers, as the MLLM-generated questions were often ambiguous or repetitive, and many answers were incorrect.

Quality Assurance and Consolidation. Human annotators may introduce controversial assumptions and biases. To ensure a broader consensus and catch ambiguous questions, we perform two rounds of quality assurance. First, each of the 360 images is randomly assigned to an annotator (from the same pool) who did not annotate the question-answer in the previous phase. This annotator is provided with the question and the image, and asked to provide an answer. After this round, we compared the answers by the two annotators for each question. We observed that the annotators

agreed on 756 question answers (70%). We identified three key disagreement sources: 1) ambiguity of whether an object should be counted as a group or split into individual components (e.g., window versus window pane as a glass object); 2) objects that partially satisfy a property (e.g., knife that is partially made of metal or black); and 3) objects with unclear definitions (e.g., container). We resolved these disagreements by another round of quality assurance, where a third annotator (different from the first two) looked at the question, answer, and the comments, and attempted to resolve the disagreement by rephrasing the questions to make them more precise, or if that was challenging, to replace them with a new question-answer pair from the same reasoning complexity level as the original question.

Benchmark Composition and Analysis. ORBIT integrates the images, questions, and final ground truth answers in a dataset containing 1,080 questions about 360 high-quality images of photographic, animated, and AI-generated types in equal proportions. Figure 3 visualizes the distribution of questions in ORBIT on the property of the object and the dimensions of the complexity of reasoning. The overall distribution across object properties is relatively balanced. We observe a larger portion of taxonomic over physical questions in the direct recognition category, and similarly, slightly more relational than functional questions in the inference category. Curiously, when creating counterfactual questions, annotators prioritized physical and taxonomic over relational and functional knowledge. We also estimated the benchmark difficulty for humans by asking two new annotators to answer 90 questions about 30 random images from ORBIT, split across reasoning levels and object properties. Their overall accuracy of 74% and an annotator agreement of 68% indicate that while the task is challenging for humans, they answer most questions correctly.

Experimental Setup

Model Selection. To ensure representative evaluation, we include a variety of non-instruction-tuned and instruction-tuned open-source VLMs, as well as a fine-tuned VLM and a closed-source model. As non-instruction-tuned open-source VLMs, we include BLIP-2 (Li et al. 2023) combined with OPT-2.7b and OPT-6.7b (Zhang et al. 2022), and Fuyu-8b (Bavishi et al. 2023). We include the instruction-tuned open-source models BLIP-2 paired with Flan T5-xxl (Chung et al. 2024), Qwen2.5-VL (3B, 7B, and 32B Instruct models) (Bai et al. 2025), and InternVL3 family (8B and 14B variants) (Zhu et al. 2025) prominent on the Hugging Face OpenVLM Leaderboard (Duan et al. 2024), and Gemma 3 (Google et al. 2025b) with 27B parameters. Our study incorporates the SpatialVLM fine-tuned version of Qwen2.5-VL for spatial relations and depth estimation in VQA (Chen et al. 2024), SpaceThinker-Qwen2.5-VL, claimed by the authors to be their most accurate fine-tuned specialized reasoning model. As a closed-source VLM, we include only GPT-4o-mini due to budget considerations (OpenAI et al. 2024). Finally, we include a baseline that samples a valid answer (0-10) uniformly randomly, i.e., at 9.09% accuracy. All models are evaluated in a zero-shot setting using standard hyperparameters. **Answer Extraction.** To extract numeric answers from

Model	Micro Acc (↑)	Macro Acc (↑)	RMSE (↓)	Mean Error (↓)	Off- By-1 (↑)
<i>Random</i>	9.09	9.09	4.47	0.00	25.62
BLIP-2 OPT (2.7B)	12.87 [†]	10.92	3.66	-2.68	35.28
BLIP-2 OPT (6.7B)	16.67 [†]	9.68	3.06	-1.56	46.11
Fuyu (8B)	19.91	11.88	2.68	-0.89	49.72
BLIP-2 Flan (11B)	15.93 [†]	12.95	3.53	-2.05	42.59
Qwen2.5 (3B)	24.91	23.55	15.30	-1.16	51.85
Qwen2.5 (7B)	38.70	<u>31.57</u>	<u>1.88</u>	-0.62	<u>70.28</u>
Qwen2.5 (32B)	39.91	34.46	1.80	-0.35	72.78
SpaceThinker (3B)	29.63	25.32	2.19	-0.89	62.50
InternVL3 (8B)	37.59	31.30	1.93	-0.70	<u>70.28</u>
InternVL3 (14B)	<u>39.72</u>	29.90	2.08	-0.91	68.61
Gemma3 (27B)	31.76	24.43	2.20	-0.14	65.28
GPT-4o mini	30.37	22.74	15.19	-0.36	64.17
<i>Model average</i>	28.16	22.39	4.62	-1.02	58.28
<i>Human 1</i>	75.56	75.15	4.22	0.64	82.22
<i>Human 2</i>	72.22	67.27	1.63	-0.24	85.56
<i>Human average</i>	73.89	71.21	2.92	0.2	83.89

Table 2: Zero-shot results on ORBIT. The highest and second-highest model results are highlighted in **bold** and underlined, respectively. (↑)/(↓) indicates that higher/lower values are better.

model outputs, we employ regular expressions for detection and perform exact string matching against ground-truth labels. Prompts were designed to facilitate this extraction by requesting only the total count (numeric) or a count followed by object lists (see Table 6). The regular expression extraction is kept flexible to obtain counts provided in textual or Roman numeral format (observed with some non-instruction-tuned models). Counts greater than ten are uninformative in the analysis of deviation from the ground-truth and therefore are considered invalid. We interpret missing outputs as a prediction of zero.

Evaluation Metrics. Following established count-based VQA benchmarks (Trott, Xiong, and Socher 2018; Acharya, Kafle, and Kanan 2018), we report multiple evaluation metrics. Our primary measure is micro *accuracy* (*Acc*). We report *macro accuracy*, where we average the accuracy scores for different counts, ranging from 0 to 10. We also report *Root-Mean-Squared Error* (*RMSE*) to quantify the typical deviation between predicted and ground-truth counts. To diagnose model bias, we include *mean error*, which reveals bias towards over- or under-counting. Furthermore, *off-by-N* accuracy (cumulative accuracy by tolerance) indicates the proximity of predictions to the correct count.

Results

How well can VLMs accurately count and reason about object properties? The results in Table 2 show that, for both the open- and closed-source categories, *most models outperform the random baseline, though performance remains well below human accuracy (28% versus 74% on average)*. The

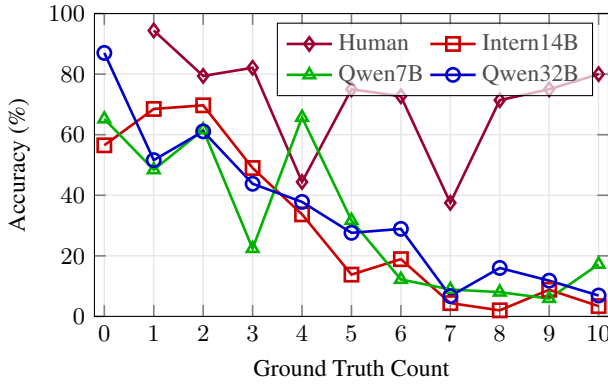


Figure 4: Accuracy per count (0-10) for human with an average (micro) accuracy of 73.89% and the top-3 best performing models: Qwen2.5-VL-Instruct (32B), InternVL3 (14B), and Qwen2.5-VL-Instruct (7B).

high RMSE across many of the models indicates substantial variance in predictions, suggesting that precise numerical grounding is challenging, even for strong VLMs. The negative mean error values suggest consistent underestimation and a general bias towards undercounting. We noted a severely imbalanced prediction distribution in the outputs of some VLMs (see Table 2 and Figure 7). When allowing one counting error, the accuracy increases to 58% on average (to 73% for the best model), which indicates that many model errors are near-misses (see Figure 8 for in-depth analysis of the top-3 best performing models). For all models, the micro accuracy is higher than the macro accuracy. We look into this difference by analyzing the accuracy across ground truth counts in Figure 4, which shows that all models have a bias towards low, more frequent counts. In contrast, the accuracy for humans is uniform in answer counts, with no apparent frequency biases.

How does performance vary across VLMs? Accuracies vary widely across all models, between 12.87% and 39.91%. The open-source Qwen2.5-VL-Instruct (32B) is the best-performing model, with the highest exact and off-by-1 accuracy, the lowest RMSE, and a low mean error. A small gap separates it from InternVL3 (14B), with the second-highest overall accuracy, and Gemma 3 (27B), which achieves the lowest mean error. In the closed-source category, the GPT-4o-mini exhibits moderate performance, with a high RMSE and low mean error. Table 3 presents results across reasoning levels, property dimensions, and image types, where the open-source Qwen2.5-VL-Instruct (7B) and (32B) variants demonstrate the strongest performance across nearly all categories. Overall, we observe that GPT-4o-mini performs consistently worse than most instruction-tuned open-source models. We also note a typical increase in performance with increasing model size within model families, though this may not always hold across architectures.

How does performance vary across reasoning levels? Based on the presented framework, we expect the progression of reasoning complexity as *recognition* < *property inference* < *counterfactual*. However, the results among the

top-tier VLMs (Qwen2.5-VL-Instruct, InternVL3, Gemma 3, and GPT-4o-mini) suggest a progression *property inference* < *recognition* < *counterfactual*. This suggests that modern VLMs still exhibit poor low-level perceptual capabilities, which aligns with several recent findings. First, Jiang et al. (2024) showed poor perceptual performance of MLLMs for fine-grained visual analysis tasks, including counting. Second, Zhang et al. (2024a) found blind spots in MLLMs with sensitivity to visual quality and distractors in the image. And, finally, Yuan et al. (2021) showed perception failures in the MetaVQA framework and highlighted the need for detailed perceptual grounding of VLMs. The lower performance on counterfactual questions is indicative of the difficulty with changes and hypotheticals and their reliance on commonsense reasoning and learned associations, areas where modern VLMs lack better grounding (Li et al. 2024). Similarly to VLMs, humans perform best on inference questions, but struggle less with counterfactual reasoning.

How does performance vary across object properties?

Among the object property dimensions, most models (as well as humans) have a stronger grasp on taxonomic and relational questions compared to physical and functional ones. This finding is in line with recent work that points out the struggle of LLMs with physical object attributes (Wang et al. 2023), physical interactions (Aroca-Ouellette et al. 2021), functional requirements (Qasemi et al. 2022), and atypical affordances (Tian et al. 2025). We note an improvement obtained by the fine-tuned SpaceThinker-Qwen2.5-VL (3B) model compared to its non-fine-tuned counterpart, Qwen2.5-VL (3B), across the four object property dimensions. This shows that besides relational questions, the other object properties also benefit from spatial tuning of Qwen2.5 (3B). We also observe that the InternVL3 models have a better grasp of taxonomic and relational questions compared to other models. The Qwen2.5-VL (7B) and (32B) model variants demonstrate consistent performance across all property types, with particular strength in physical and functional questions compared to others. In contrast, the non-instruction-tuned models face difficulty across all properties, stressing their weakness in visual object reasoning.

How does performance vary across image types? We observe a consistently higher performance for AI-generated and animated images, compared to photographic images. We hypothesize that this is due to the visually cleaner and less cluttered nature of AI-generated and animated images compared to the complex and noisy real-world scenes in photographic images. This finding aligns with those of previous benchmarks (Johnson et al. 2017; Hudson and Manning 2019). Moreover, we note that animated images are easier for most models than AI-generated images, possibly because AI-generated images may have poor focus and may include implausible objects, such as a half-cut glass floating in the air. The trend between the image difficulty *animated* < *AI-generated* < *photographic* is also clear in humans, which indicates that questions about photographic images may be hardest and possibly contain remaining ambiguity.

Can densely annotated datasets be used to automatically scale up ORBIT? Visual Genome (VG) (Krishna et al. 2017) is a popular dataset with high-quality structured con-

Model	Reasoning Complexity			Object Properties				Image Types		
	Direct Recognition	Property Inference	Counter-factual	Physical	Taxonomic	Functional	Relational	Photographic	Animated	AI Gen.
BLIP-2 OPT (2.7B)	10.83	13.06	14.72	11.48	14.41	10.91	13.78	9.17	19.44	10.00
BLIP-2 OPT (6.7B)	16.67	18.06	15.28	16.39	16.52	14.09	19.08	14.17	21.11	14.72
Fuyu (8B)	18.33	22.78	18.61	17.21	17.42	19.55	25.44	16.94	23.89	18.89
BLIP-2 Flan (11B)	18.33	18.61	10.83	14.34	16.82	13.64	18.02	11.67	20.00	16.11
Qwen2.5 (3B)	26.11	29.17	19.44	21.31	29.43	17.73	28.27	20.28	27.78	26.67
Qwen2.5 (7B)	42.78	44.17	29.17	35.66	42.34	32.73	<u>41.70</u>	32.22	40.83	43.06
Qwen2.5 (32B)	<u>39.17</u>	<u>43.06</u>	37.50	<u>33.61</u>	<u>44.44</u>	38.18	41.34	31.94	45.00	<u>42.78</u>
SpaceThinker (3B)	34.44	30.28	24.17	25.00	37.24	19.55	32.51	25.56	31.11	32.22
InternVL3 (8B)	38.89	41.94	31.94	33.20	42.34	26.82	44.17	28.89	43.61	40.28
InternVL3 (14B)	42.78	42.22	<u>34.17</u>	30.33	48.05	36.82	40.28	32.22	48.61	38.33
Gemma3 (27B)	33.89	35.56	25.83	26.23	34.53	28.64	35.69	27.78	36.39	31.11
GPT-4o mini	28.89	33.61	28.61	21.31	34.23	25.00	37.81	24.44	38.89	27.78
<i>Model average</i>	29.34	31.04	24.18	23.83	31.48	23.63	31.50	22.94	33.05	28.49
<i>Human 1</i>	73.33	80.00	73.33	58.33	92.00	71.43	80.00	63.33	83.33	80.00
<i>Human 2</i>	66.67	76.67	73.33	58.33	80.00	76.19	75.00	60.00	83.33	73.33
<i>Human average</i>	70.00	78.33	73.33	58.33	86.00	73.81	77.50	61.66	83.33	76.66

Table 3: Accuracy results for each model on ORBIT across reasoning levels, object property dimensions, and image types. The highest and second highest model results are highlighted in **bold** and underlined, respectively.

nections between image regions, language descriptions, and WordNet (Miller 1995) synsets. To investigate whether the annotations of VG can support the generation of large-scale instantiations of ORBIT, we devised a procedure that generates taxonomic questions by manipulating the WordNet synsets. This experiment exposed three limitations: lack of contextualization of classes (e.g., kitchen utensil instead of a bowl in Figure 11-left), incorrect questions or answers (e.g., about uncountable objects like grass in Figure 11-right), and classes in the WordNet hierarchy that are not overly specific (e.g., derby horse race) or generic (e.g., entity). Thus, while every image in VG enables many taxonomic questions to be created, it remains challenging to automatically distinguish high- from low-quality question-answer pairs. More fundamentally, creating question-answer pairs for other object properties (e.g., functional) and reasoning types (e.g., counterfactual) is hindered by the absence of annotation. While LLMs can be employed to generate questions for these categories, we established that these questions and answers are often incorrect or ambiguous (e.g., suggesting that buildings, doors, and windows can all provide shelter). In conclusion, we find that densely annotated image datasets remain insufficient to generate high-quality large-scale versions of ORBIT. Yet, they could potentially be used to speed up human annotation by providing an initial set of samples or for distant supervision of VQA models.

Conclusions

This paper developed an evaluation framework for evaluating object-centric reasoning in images. The framework considers three distinct image types (photographic, animated, and AI-generated), three reasoning levels (direct recognition, property inference, counterfactual), and four prop-

erty types (physical, taxonomic, functional, relational). We instantiated this framework into ORBIT, a VQA benchmark with over 1,000 questions for 360 images, split uniformly across the evaluation dimensions. Experiments with 12 state-of-the-art VLMs revealed low accuracy, with most models performing far below humans, and the best only achieving 40% accuracy. VLMs struggle particularly with realistic (photographic) images, counterfactual reasoning about physical and functional properties, and infrequent counts over 5. Humans also struggle with photographic images and physical properties, but excel at counterfactual questions and have no frequency effects on counts.

Three key limitations should be addressed in future work. First, as generative AI still suffers from limited accuracy and diversity in autonomous question generation, which makes *scaling up object abstraction benchmarks require substantial human effort*. Novel approaches, such as metamorphic testing (Yuan et al. 2021), are necessary to grow ORBIT systematically in size and coverage of additional object properties, question types beyond counting, and open-ended answers. Second, since annotators are unrestricted in their question design, they may *introduce linguistic ambiguity*, leading to disagreements across annotators (e.g., whether zebras are considered black animals). While we addressed ambiguity in an explicit quality assurance step, during which sources of disagreements are analyzed and converted into more precise guidelines, some disagreements remain. Future work should develop generalizable, well-understood guidelines for object abstraction and reasoning. Finally, while ORBIT points to fundamental limitations of 12 popular and diverse VLMs, *the set of baselines is inherently incomplete*. Future work should explore additional specialized reasoners beyond SpatialVLM, e.g., mixtures of experts (Lin et al. 2024) and derivation of object schemas (Hsu et al. 2024).

Acknowledgements

This paper is based on Abhishek Kolari’s MSc AI project at Vrije Universiteit Amsterdam with the same title. MK and FI were funded by the AiNed project *Human-Centric AI Agents with Common Sense* supported by the Dutch Organisation for Scientific Research (NWO), under grant no. NGF.1607.22.044. FdH was funded by the Hybrid Intelligence Centre, a 10-year programme supported by the Dutch Ministry of Education, Culture and Science through NWO (grant no. 024.004.022). The evaluations were performed on the DAS-6 cluster (Bal et al. 2016).

References

- Acharya, M.; Kaffle, K.; and Kanan, C. 2018. TallyQA: Answering Complex Counting Questions. *arXiv:1810.12440*.
- Aguiar, A.; and Baillargeon, R. 1999. 2.5-month-old infants’ reasoning about when objects should and should not be occluded. *Cognitive psychology*, 39(2): 116–157.
- Anthropic. 2025. Claude 3.7 Sonnet and Claude Code. *Anthropic News*.
- Antol, S.; Agrawal, A.; Lu, J.; Mitchell, M.; Batra, D.; Zitnick, C. L.; and Parikh, D. 2015. Vqa: Visual question answering. In *Proceedings of the IEEE international conference on computer vision*, 2425–2433.
- Aroca-Ouellette, S.; Paik, C.; Roncone, A.; and Kann, K. 2021. Prost: Physical reasoning of objects through space and time. *arXiv preprint arXiv:2106.03634*.
- Bai, S.; Chen, K.; Liu, X.; Wang, J.; Ge, W.; Song, S.; Dang, K.; Wang, P.; Wang, S.; Tang, J.; Zhong, H.; Zhu, Y.; Yang, M.; Li, Z.; Wan, J.; Wang, P.; Ding, W.; Fu, Z.; Xu, Y.; Ye, J.; Zhang, X.; Xie, T.; Cheng, Z.; Zhang, H.; Yang, Z.; Xu, H.; and Lin, J. 2025. Qwen2.5-VL Technical Report. *arXiv preprint arXiv:2502.13923*.
- Bal, H.; Epema, D.; De Laat, C.; Van Nieuwpoort, R.; Romein, J.; Seinstra, F.; Snoek, C.; and Wijshoff, H. 2016. A medium-scale distributed system for computer science research: Infrastructure for the long term. *Computer*, 49(5): 54–63.
- Bavishi, R.; Elsen, E.; Hawthorne, C.; Nye, M.; Odena, A.; Somani, A.; and Tasirlar, S. 2023. Fuyu-8b: A multi-modal architecture for ai agents. *URL: https://www.adept.ai/blog/fuyu-8b*.
- Chen, B.; Xu, Z.; Kirmani, S.; Ichter, B.; Sadigh, D.; Guibas, L.; and Xia, F. 2024. SpatialVLM: Endowing Vision-Language Models with Spatial Reasoning Capabilities. In *Proceedings of the IEEE/CVF Conference on Computer Vision and Pattern Recognition (CVPR)*, 14455–14465.
- Chung, H. W.; Hou, L.; Longpre, S.; Zoph, B.; Tay, Y.; Fedus, W.; Li, Y.; Wang, X.; Dehghani, M.; Brahma, S.; et al. 2024. Scaling instruction-finetuned language models. *Journal of Machine Learning Research*, 25(70): 1–53.
- Dodge, J.; Sap, M.; Marasović, A.; Agnew, W.; Ilharco, G.; Groeneveld, D.; Mitchell, M.; and Gardner, M. 2021. Documenting large webtext corpora: A case study on the colossal clean crawled corpus. *arXiv preprint arXiv:2104.08758*.
- Duan, H.; Yang, J.; Qiao, Y.; Fang, X.; Chen, L.; Liu, Y.; Dong, X.; Zang, Y.; Zhang, P.; Wang, J.; et al. 2024. Vlmevalkit: An open-source toolkit for evaluating large multi-modality models. In *Proceedings of the 32nd ACM International Conference on Multimedia*, 11198–11201.
- Fields, C. 2016. How Humans Recognize Objects: Segmentation, Categorization and Individual Identification.
- Fleming, R. W. 2017. Material perception. *Annual review of vision science*, 3(1): 365–388.
- Frohberg, J.; and Binder, F. 2021. Crass: A novel data set and benchmark to test counterfactual reasoning of large language models. *arXiv preprint arXiv:2112.11941*.
- Google; Team, G.; Anil, R.; Borgeaud, S.; Alayrac, J.-B.; Yu, J.; Soricut, R.; Schalkwyk, J.; Dai, A. M.; Hauth, A.; Millican, K.; et al. 2025a. Gemini: a family of highly capable multimodal models. *arXiv preprint arXiv:2312.11805*.
- Google; Team, G.; Kamath, A.; Ferret, J.; Pathak, S.; Vieillard, N.; Merhej, R.; Perrin, S.; Matejovicova, T.; Ramé, A.; Rivière, M.; et al. 2025b. Gemma 3 technical report. *arXiv preprint arXiv:2503.19786*.
- Goyal, Y.; Khot, T.; Summers-Stay, D.; Batra, D.; and Parikh, D. 2017. Making the v in vqa matter: Elevating the role of image understanding in visual question answering. In *Proceedings of the IEEE conference on computer vision and pattern recognition*, 6904–6913.
- Heindorf, S.; Scholten, Y.; Wachsmuth, H.; Ngonga Ngomo, A.-C.; and Potthast, M. 2020. Causenet: Towards a causality graph extracted from the web. In *Proceedings of the 29th ACM international conference on information & knowledge management*, 3023–3030.
- Hoffman, D. D.; and Richards, W. A. 1987. Parts of recognition. In *Readings in Computer Vision*, 227–242. Elsevier.
- Hsu, J.; Mao, J.; Tenenbaum, J. B.; Goodman, N. D.; and Wu, J. 2024. What Makes a Maze Look Like a Maze? *arXiv preprint arXiv:2409.08202*.
- Hudson, D. A.; and Manning, C. D. 2019. Gqa: A new dataset for real-world visual reasoning and compositional question answering. In *Proceedings of the IEEE/CVF conference on computer vision and pattern recognition*, 6700–6709.
- Ilievski, F.; Oltramari, A.; Ma, K.; Zhang, B.; McGuinness, D. L.; and Szekely, P. 2021. Dimensions of commonsense knowledge. *Knowledge-Based Systems*, 229: 107347.
- Jiang, Y.; Sun, K.; Sourati, Z.; Ahrabian, K.; Ma, K.; Ilievski, F.; Pujara, J.; et al. 2024. Marvel: Multidimensional abstraction and reasoning through visual evaluation and learning. *Advances in Neural Information Processing Systems*, 37: 46567–46592.
- Johnson, J.; Hariharan, B.; Van Der Maaten, L.; Fei-Fei, L.; Lawrence Zitnick, C.; and Girshick, R. 2017. Clevr: A diagnostic dataset for compositional language and elementary visual reasoning. In *Proceedings of the IEEE conference on computer vision and pattern recognition*, 2901–2910.
- Kraaijveld, K.; Jiang, Y.; Ma, K.; and Ilievski, F. 2025. Columbus: Evaluating cognitive lateral understanding through multiple-choice rebuses. In *Proceedings of*

- the AAAI Conference on Artificial Intelligence, volume 39, 4410–4418.
- Krishna, R.; Zhu, Y.; Groth, O.; Johnson, J.; Hata, K.; Kravitz, J.; Chen, S.; Kalantidis, Y.; Li, L.-J.; Shamma, D. A.; et al. 2017. Visual genome: Connecting language and vision using crowdsourced dense image annotations. *International journal of computer vision*, 123: 32–73.
- Kurtz, K. J.; and Silliman, D. C. 2021. Object understanding: Investigating the path from percept to meaning. *Acta Psychologica*, 216: 103307.
- Leslie, A. M.; and Keeble, S. 1987. Do six-month-old infants perceive causality? *Cognition*, 25(3): 265–288.
- Li, J.; Li, D.; Savarese, S.; and Hoi, S. 2023. Blip-2: Bootstrapping language-image pre-training with frozen image encoders and large language models. In *International conference on machine learning*, 19730–19742. PMLR.
- Li, Y.; Tian, W.; Jiao, Y.; Chen, J.; and Jiang, Y.-G. 2024. Eyes can deceive: Benchmarking counterfactual reasoning abilities of multi-modal large language models. *arXiv e-prints*, arXiv:2404.
- Lin, B.; Tang, Z.; Ye, Y.; Cui, J.; Zhu, B.; Jin, P.; Huang, J.; Zhang, J.; Pang, Y.; Ning, M.; et al. 2024. Moe-llava: Mixture of experts for large vision-language models. *arXiv preprint arXiv:2401.15947*.
- Lipton, J. S.; and Spelke, E. S. 2004. Discrimination of large and small numerosities by human infants. *Infancy*, 5(3): 271–290.
- Lobben, M. 2012. Semantic classification in category-specific semantic impairments reflected in the typology of Bantu noun class systems. In *Selected proceedings of the 41st Annual Conference on African Linguistics: African Languages in Contact. Cascadilla Proceedings Project, Somerville, MA*, 361–404.
- Lu, P.; Mishra, S.; Xia, T.; Qiu, L.; Chang, K.-W.; Zhu, S.-C.; Tafjord, O.; Clark, P.; and Kalyan, A. 2022. Learn to explain: Multimodal reasoning via thought chains for science question answering. *Advances in Neural Information Processing Systems*, 35: 2507–2521.
- Marino, K.; Rastegari, M.; Farhadi, A.; and Mottaghi, R. 2019. Ok-vqa: A visual question answering benchmark requiring external knowledge. In *Proceedings of the IEEE/cvf conference on computer vision and pattern recognition*, 3195–3204.
- Mathew, M.; Karatzas, D.; and Jawahar, C. 2021. Docvqa: A dataset for vqa on document images. In *Proceedings of the IEEE/CVF winter conference on applications of computer vision*, 2200–2209.
- McCloskey, M.; Washburn, A.; and Felch, L. 1983. Intuitive physics: the straight-down belief and its origin. *Journal of Experimental Psychology: Learning, Memory, and Cognition*, 9(4): 636.
- Miller, G. A. 1995. WordNet: a lexical database for English. *Communications of the ACM*, 38(11): 39–41.
- Mirman, D.; Landrigan, J.-F.; and Britt, A. E. 2017. Taxonomic and thematic semantic systems. *Psychological bulletin*, 143(5): 499.
- OpenAI; Hurst, A.; Lerer, A.; Goucher, A. P.; Perelman, A.; Ramesh, A.; Clark, A.; Ostrow, A.; Welihinda, A.; Hayes, A.; Radford, A.; et al. 2024. Gpt-4o system card. *arXiv preprint arXiv:2410.21276*.
- Qasemi, E.; Ilievski, F.; Chen, M.; and Szekely, P. 2022. PaCo: Preconditions Attributed to Commonsense Knowledge. In Goldberg, Y.; Kozareva, Z.; and Zhang, Y., eds., *Findings of the Association for Computational Linguistics: EMNLP 2022*, 6781–6796. Abu Dhabi, United Arab Emirates: Association for Computational Linguistics.
- Singh, A.; Natarajan, V.; Shah, M.; Jiang, Y.; Chen, X.; Batra, D.; Parikh, D.; and Rohrbach, M. 2019. Towards vqa models that can read. In *Proceedings of the IEEE/CVF conference on computer vision and pattern recognition*, 8317–8326.
- Speer, R.; Chin, J.; and Havasi, C. 2017. Conceptnet 5.5: An open multilingual graph of general knowledge. In *Proceedings of the AAAI conference on artificial intelligence*, volume 31.
- Spelke, E. S.; and Kinzler, K. D. 2007. Core knowledge. *Developmental science*, 10(1): 89–96.
- Tandon, N.; de Melo, G.; and Weikum, G. 2017. WebChild 2.0 : Fine-Grained Commonsense Knowledge Distillation. In Bansal, M.; and Ji, H., eds., *Proceedings of ACL 2017, System Demonstrations*, 115–120. Vancouver, Canada: Association for Computational Linguistics.
- Tian, Y.; Ravichander, A.; Qin, L.; Bras, R. L.; Marjeh, R.; Peng, N.; Choi, Y.; Griffiths, T. L.; and Brahman, F. 2025. MacGyver: Are Large Language Models Creative Problem Solvers? *arXiv:2311.09682*.
- Tong, S.; Liu, Z.; Zhai, Y.; Ma, Y.; LeCun, Y.; and Xie, S. 2024. Eyes wide shut? exploring the visual shortcomings of multimodal llms. In *Proceedings of the IEEE/CVF Conference on Computer Vision and Pattern Recognition*, 9568–9578.
- Trott, A.; Xiong, C.; and Socher, R. 2018. Interpretable Counting for Visual Question Answering. *arXiv:1712.08697*.
- Wang, Y. R.; Duan, J.; Fox, D.; and Srinivasa, S. 2023. NEWTON: Are large language models capable of physical reasoning? *arXiv preprint arXiv:2310.07018*.
- Wang, Z.; and Wu, L. 2023. Theoretical analysis of the inductive biases in deep convolutional networks. *Advances in Neural Information Processing Systems*, 36: 74289–74338.
- Xu, L.; Huang, H.; and Liu, J. 2021. Sutd-trafficqa: A question answering benchmark and an efficient network for video reasoning over traffic events. In *Proceedings of the IEEE/CVF conference on computer vision and pattern recognition*, 9878–9888.
- Yu, W.; Jiang, M.; Clark, P.; and Sabharwal, A. 2023. Ifqa: A dataset for open-domain question answering under counterfactual presuppositions. *arXiv preprint arXiv:2305.14010*.
- Yuan, Y.; Wang, S.; Jiang, M.; and Chen, T. Y. 2021. Perception matters: Detecting perception failures of vqa models using metamorphic testing. In *Proceedings of the IEEE/CVF Conference on Computer Vision and Pattern Recognition*, 16908–16917.

Zhang, J.; Hu, J.; Khayatkhoei, M.; Ilievski, F.; and Sun, M. 2024a. Exploring perceptual limitation of multimodal large language models. *arXiv preprint arXiv:2402.07384*.

Zhang, J.; Khayatkhoei, M.; Chhikara, P.; and Ilievski, F. 2025. Mllms know where to look: Training-free perception of small visual details with multimodal llms. *arXiv preprint arXiv:2502.17422*.

Zhang, L.; Zhai, X.; Zhao, Z.; Zong, Y.; Wen, X.; and Zhao, B. 2024b. What if the tv was off? examining counterfactual reasoning abilities of multi-modal language models. In *Proceedings of the IEEE/CVF Conference on Computer Vision and Pattern Recognition*, 21853–21862.

Zhang, S.; Roller, S.; Goyal, N.; Artetxe, M.; Chen, M.; Chen, S.; Dewan, C.; Diab, M.; Li, X.; Lin, X. V.; et al. 2022. Opt: Open pre-trained transformer language models. *arXiv preprint arXiv:2205.01068*.

Zhu, J.; Wang, W.; Chen, Z.; Liu, Z.; Ye, S.; Gu, L.; Tian, H.; Duan, Y.; Su, W.; Shao, J.; et al. 2025. Internvl3: Exploring advanced training and test-time recipes for open-source multimodal models. *arXiv preprint arXiv:2504.10479*.

Appendix

Benchmark Examples

Image Types

Figure 5 shows additional examples from ORBIT for three image types: Photographic, Animated, and AI-generated.

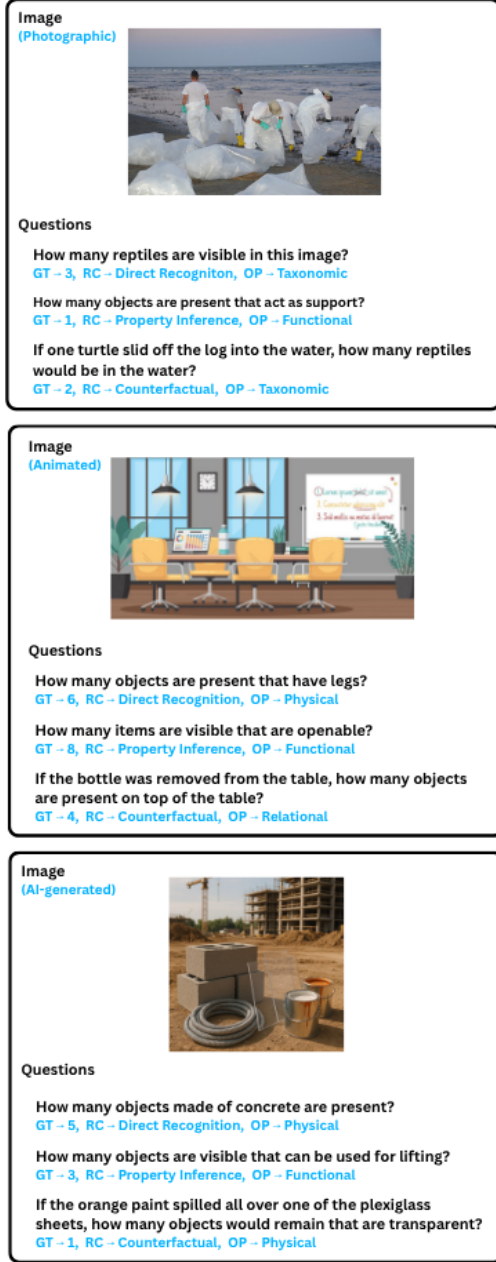


Figure 5: Examples from ORBIT, for three image types: Photographic (top-left), Animated (top-right), and AI-generated (bottom). Text highlighted in blue is information stored in the benchmark and not passed to the model during evaluation. GT stands for ground truth, RC is reasoning complexity, and OP for object properties.

Object Property Dimensions

Table 4 shows examples of questions present per object property dimension.

Dimensions	Question Examples
Physical	How many objects made of wood are present? How many objects are present that are transparent? How many objects in the background are present that have legs?
Taxonomic	How many mammals are visible in the image? How many furniture items are present in the room? How many tools are visible in the image?
Functional	How many objects with the primary purpose of illumination can be seen? Count the number of breakable items? Count the number of items that are battery powered?
Relational	How many objects are visible that are attached to the wall or ceiling? How many reptilian couples, at maximum, are present?

Table 4: Question examples for the different object property dimensions: physical, taxonomic, functional, and relational.

Reasoning Complexity

Table 5 shows examples of the questions asked at the different reasoning levels. Direct recognition has questions from the taxonomical and physical object property dimensions; property inference has questions from the functional and relational dimensions; and counterfactual reasoning has questions from any of the four property dimensions.

Prompt Strategies

Question Generation

We pass a standard prompt template to any of the three MLLMs: GPT-4o, Claude 3.7 Sonnet, and Gemini 2.0 Flash to generate questions, which are then used to inspire humans to generate new questions manually. The template is as follows:

{IMG} Generate three questions per prompt for this image with answers for each prompt. Prompt 1 deals with physical/taxonomic properties; prompt 2 deals with functional/relational properties; and prompt 3 deals with counterfactual reasoning. All need to be counting questions; be creative. You do not need to stick to the same questions.

Output Formatting

Table 6 displays the prompt templates used on instruction-tuned and non-instruction-tuned models to extract outputs

Complexity	Dimension	Question Example
Direct Recognition	physical taxonomic	How many objects made of wood are present? How many mammals are visible in the image?
Property Inference	functional relational	Count the number of breakable items? How many objects are visible that are attached to the wall or ceiling?
Counterfactual	physical	If one of the metal objects were replaced by a wooden object, how many wooden objects would be there in the image?
	taxonomic	If one person leaves the cleaning group, how many mammals would remain?
	functional	If the two bedside lamps were removed, how many objects are present that need electricity?
	relational	If the signages were removed, how many objects would be present that hang from the ceiling?

Table 5: Question examples for the different reasoning complexity levels that is direct recognition, property inference, and counterfactual.

in a specific format. Instruction-based models are also asked for a list of objects detected and considered for the count, which is currently not directly evaluated.

AI-Generated images

Table 8 shows the prompt examples used while generating AI-based images for different image themes.

Ground Truth Distribution

For the total number of 1,080 questions, the ground truth distribution for all the counts ranging from 0 to 10 is shown in Figure 6.

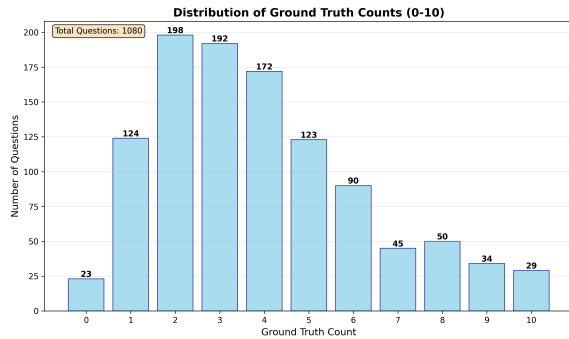


Figure 6: Ground Truth distribution for all counts ranging from 0 to 10.

Image Theme Tags

During image collection (Figure 2), to direct our search we made use of image theme tags inspired by the tags used in curating the Macgyver dataset (Tian et al. 2025). Table 7 shows the list of 26 unique image theme tags used for the curation of ORBIT. The process of selecting a tag was influenced by the chance of a particular theme having more variety of objects. The tags used for the MacGyver dataset were plentiful out of which 15 tags were in common, namely: bedroom, kitchen, library, meeting room, gym, wardrobe,

garage, classroom, beach cleanup, camping, construction, gardening, zoo, park, and farm. The remaining 9 tags came into fruition off our own efforts.

Inductive Bias

The BLIP2 model series consistently defaults to specific output values, showing possibilities of inductive bias present in the models. The OPT 2.7B variant goes for the count 1, the OPT 6.7B variant produces either 1 or 3 as the output, and the FLan T5 xxL gives an output as 0 or no value or an answer not abiding by the required format (numeric value), resulting in a final output as 0 set according to our answer extraction method. The frequency distribution of these outputs is shown in Figure 7. We tried adjusting prompts and decoding parameters, such as the number of maximum new tokens, but none helped mitigate the issue, highlighting the potential inductive biases present in models (Wang and Wu 2023; Kraaijveld et al. 2025).

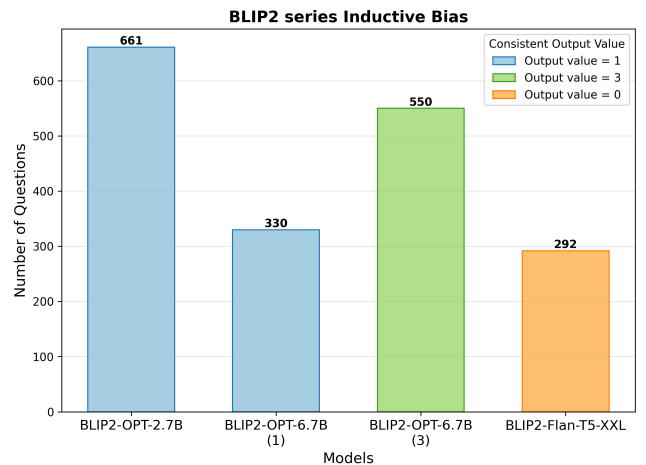


Figure 7: BLIP2 model series inductive bias plot, consistently defaulting to specific output values.

Category	Prompt Template
Non-Instruction-tuned models	$\{IMG\}$ Question: $\{question\}$ Provide only the total number. Answer:
Instruction-tuned models	$\{IMG\}$ $\{question\}$ Your response MUST be in the following format and nothing else: <NUMBER> [<OBJECT1>, <OBJECT2>, <OBJECT3>, ...]

Table 6: Prompt template used to extract output in a specific format from the model for non-instruction-tuned and instruction-tuned models. $\{IMG\}$ and $\{question\}$ are the placeholders for the image and question, respectively.

Indoors/Household	Neutral	Outdoors
bedroom	tools	beach cleanup
home setup	tech	camping
kitchen	garage	construction
library	classroom	gardening
laboratory		biking
meeting room		market
gym		zoo
salon		urban
wardrobe		park
		picnic
		farm
		driveway
		bustop

Table 7: The 15 tags (i.e., locations and activities) taken from the MacGyver dataset (Tian et al. 2025), extended with 11 of our own, for a total of 26 unique image themes. They are broadly divided into Indoors/Household, Neutral, and Outdoors.

Cumulative Accuracies with Tolerance

The soft off-by-1 accuracy metric, which has a baseline of 25.62%, reveals relatively better improvements (47.16% gap with the best model) among the larger instruction-tuned models. Even though the models predictions are often nearly correct, this metric highlights the difficulty in precise numeric predictions by VLMs. The cumulative accuracy for tolerance values 0, 1, and 2 is shown in Figure 8 for the top-performing models in their categories and the average of the human evaluators.

Visual Depiction of Errors

ORBIT requires models to have good low-level perception and the ability to perform fine-grained analysis. A case study on the errors models typically make is visually depicted using an image of *photographic* type. Figure 9 shows an instance from ORBIT, with the ground truth values provided after the question in the yellow cell and the depiction of object counts through green bounding boxes. The bounding boxes are manually annotated on the images using Canva.¹ To showcase the output of the model, we consider the open-source model, Gemma 3 (27B), for this study. Figure 10 dis-

¹<https://www.canva.com/>

plays the model’s predicted values and the probable object selection, with green (correct) and red (incorrect) bounding boxes based on detailed reasoning explicitly requested for this image.

For the first question, the model outputs 5, as it misses the sparrow that is partially occluded but still visible to the human eye. In the second question, the model outputs 6, as it tends to over-count the row of chairs due to the challenging angle at which the picture is captured. In the final question, the model outputs 2, reasoning that there are three birds (excluding the partially visible one) on the right sitting together on one railing, leaving two birds on the left. But in the ground truth, the bird positioned on the extreme right is sitting on a different metal frame. Based on the model’s answer to the first question, its reasoning is consistent with the third question’s answer.

The model fails to detect objects that are partially hidden, indicating weak low-level perception. It misinterprets perspective and geometric layout and struggles to distinguish objects that are closely clustered together. Despite the incorrect answers, the model’s internal reasoning is logically consistent. This study highlights the importance of evaluating not only the final count, but also the quality of visual grounding and traceability of reasoning for tasks like those

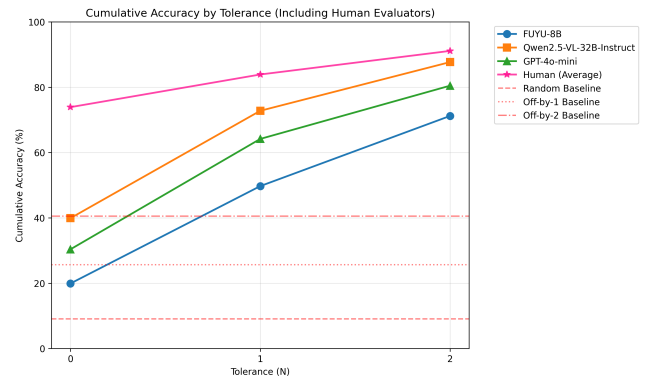


Figure 8: Cumulative accuracies for tolerance levels 0, 1, and 2. The top-performing models from the following categories are shown: open-source non-instruction VLM (Fuyu-8B), open-source instruction VLM (Qwen2.5-VL-32B-Instruct), closed-source VLM (GPT-4o mini), the human evaluators average and the random chance baselines for tolerance levels 0 (9.09%), 1 (25.62%), and 2 (40.50%).

Image Theme	Prompt Example
Campsite settings (Outdoors)	Create image Generate a photorealistic dusk campsite scene with 5 tents, a few of them illuminated from within, a controlled campfire with 3 people sitting on logs around it and a dog sleeping nearby, hiking backpacks leaning against a nearby tree, a lantern hanging from a branch, and stars beginning to appear in the darkening sky. Include a mountain silhouette in the background. Strictly keep the count of total objects in the image to a maximum of 10.
Gym (Indoors/Household)	Create image Generate a photorealistic image of a gym scene with sports equipment. Let the gym contain 3 treadmills, 2 elliptical machines, a few kettlebells on the floor, 2 resistance bands hanging on the wall, and a bench press rack. Let it be a realistic setting with 2 humans working out, one person on the treadmill and another person on the elliptical machine. The gym can have a clock and TV hanging on the wall somewhere showing a workout video. Include large windows with natural light and a small plant in the corner. Strictly keep count of total objects in the image to a maximum of 10.
Beach cleanup (Outdoors)	Generate a photorealistic image of a beach cleanup scene with 4 volunteers in bright t-shirts collecting trash at sunset in the backdrop. Let the trash include these objects: 5 glass bottles, 6 trash bags (one in each hand of a volunteer and 2 placed near the ground), a collection bin, reusable gloves, and garbage pickers. Let it be a realistic setting, having the ocean with gentle waves in the background. Strictly keep the count of total objects in the image to a maximum of 10.
Garage (Neutral)	Create image Create a photorealistic image of a vehicle garage scene during a vehicle maintenance session. Show 3 cars, one car on a hydraulic lift with its hood open, 2-3 essential tools spread on a workbench, an oil change in progress, spare parts in organised containers, and a service manual. Let the setting be realistic with ceiling lights for the garage, let the car being serviced be in good condition, and let the other two cars in the background be scrap and old, which need to be rebuilt with loose tires leaning next to them. Let one person work on the car that is being serviced and the other person in the backdrop next to the other 2 cars. Strictly keep count of total objects in the image to a maximum of 10.
Kitchen (Indoors/Household)	Create image Generate an image of a kitchen countertop during the preparation of a complex dish. Show fresh ingredients arranged in 3 small ceramic bowls, a wooden cutting board with chopped herbs, a professional knife set, a simmering pot on the stove, a recipe book, a glass filled with water, and 2 people collaborating on the cooking. Include details like steam, a kitchen sink next to the stove, and ambient kitchen lighting. Let it be a realistic setting. Strictly keep the count of total objects in the image to a maximum of 10.

Table 8: Prompt examples used to generate AI images across different themes, along with corresponding tags (shown in brackets) used in constructing the MacGyver dataset. Prompts with the **Create Image** tool are generated using GPT-4o, while those without it are created with Grok 3.

in ORBIT, providing potential for future work.

Human Evaluation

An analysis of human answers indicates that the sources of incorrect responses or disagreements between annotators could be one of the following: 1) Ambiguity in image context: Some mistakes are because of partially visible objects, as people were unsure whether to count them. 2) Uncertainty in definitions: Some mistakes appear from uncertainty in the definition of objects. For instance, it was unclear to human evaluators whether lamps should be considered electronic devices, what qualifies as a metal object, or which items are included when asked about objects with arms. While we agreed on these guidelines between the original annotators,

this was not used to instruct the human evaluators. 3) Lack of attention: We also observed some mistakes in relatively straightforward questions, which we attribute to humans not examining the image carefully.

This analysis suggests that human performance could be improved in the future by providing clear guidance for questions on the first and second issues. As a result, we would expect higher accuracy and agreement among human annotators for the first two error categories.

VG-based Dataset Curation

Figure 11 shows two examples of question-answer pairs generated automatically from Visual Genome.

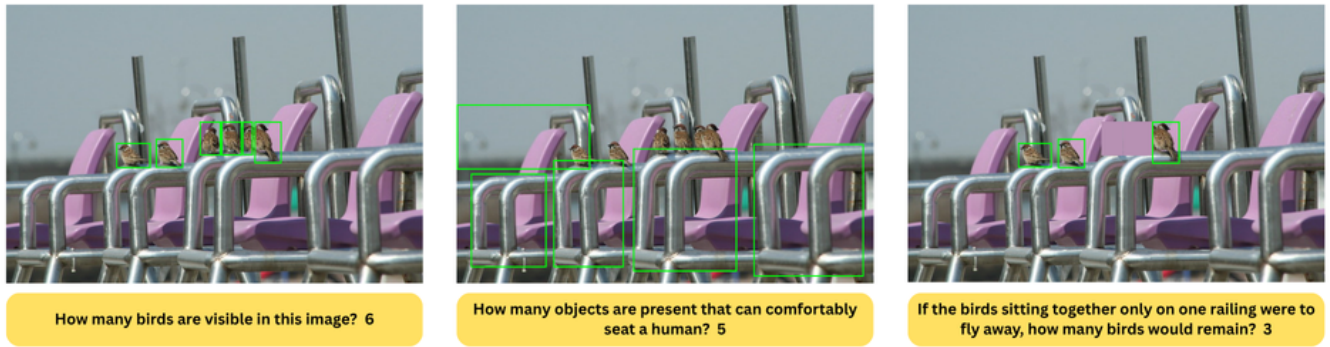


Figure 9: Questions follow the reasoning complexity order, direct recognition to counterfactual (left to right) for a photographic image with the ground truth values and the object counts visually depicted by green bounding boxes.



Figure 10: Gemma 3 model output values and the visual depiction of possible correct and incorrect detections.

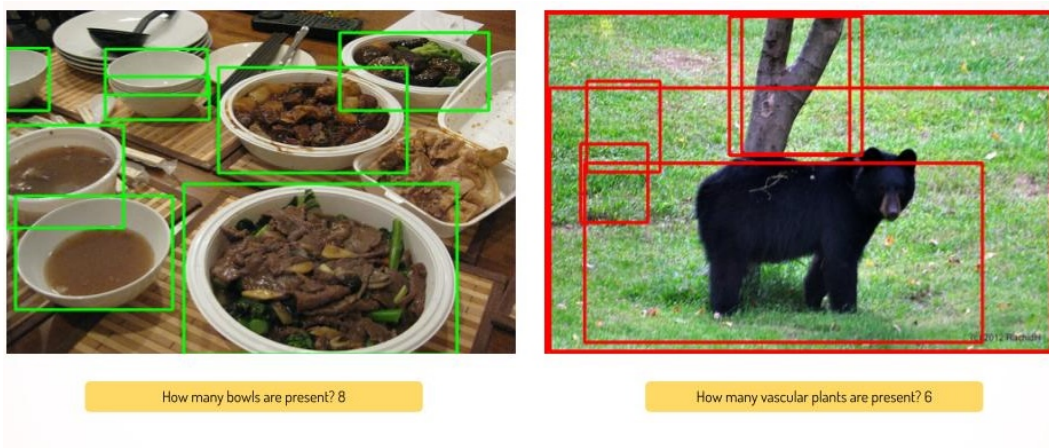


Figure 11: **Left:** A successful example of a question generated using Visual Genome. **Right:** An unsuccessful example, where multiple objects are assigned to a single tree and a single patch of grass, leading to an incorrect answer.